Different methods used to form oxygen reducing biocathodes lead to different biomass quantities, bacterial communities, and electrochemical kinetics

Mickaël Rimboud, mohamed Barakat, Alain Bergel, Benjamin Erable

Different methods used to form oxygen reducing biocathodes lead to different biomass quantities, bacterial communities, and electrochemical kinetics

Mickaël Rimboud [a,b], Mohamed Barakat [b], Alain Bergel [a], Benjamin Erable [a,*]

[a] Laboratoire de Génie Chimique, CNRS-Université de Toulouse, 4 Allée Emile Monso, 31432 Toulouse Cedex 04, France
[b] Laboratoire d'Ecologie Microbienne de la Rhizosphère et des Environnements Extrêmes (LEMIRE), BIAM, UMR 7265, CEA-CNRS-Aix Marseille Université, CEA Cadarache, 13108 Saint Paul Lez Durance, France

A B S T R A C T

Six biocathodes catalyzing oxygen reduction were designed from the same environmental inoculum but using three different methods. Two were formed freely at open circuit potential, two using conventional aerobic polarization at -0.2 V/SCE and two by reversion of already established acetate-fed bioanodes. Observation of the biofilms by SEM and epifluorescence microscopy revealed that reversible bioelectrodes had the densest biofilms. Electrochemical characterization revealed two different redox systems for oxygen reduction, at -0.30 and $+0.23$ V/SCE. The biocathodes formed under aerobic polarization gave higher electrocalatytic performance for O_2 reduction, due to production of the redox systems at $+0.23$ V/SCE. Analyses of the bacterial communities on the biocathodes by 16S-rRNA pyrosequencing showed different selection (or enrichment) of microorganisms depending on the method used. This study highlights how the method chosen for designing oxygen biocathodes can affect the cathode coverage, the selection of bacterial populations and the electrochemical performance.

1. Introduction

The implementation of microbial fuel cells (MFCs) that include electroactive biofilms as catalysts on both anode and cathode is currently hindered by the low performance of oxygen reducing (OR) biocathodes compared to bioanodes. The poor availability of oxygen in the aqueous media (0.24 mM at pH 7, 20 °C) and the lower quantity of biomass gathered on the electrode were among the factors explaining the poor performances of OR-biocathodes compared to those of bioanodes [1,2]. The absence of a carbon source/substrate in the medium, intended to favor the extraction of electrons from the cathode rather than the catabolic oxidation of the substrate, led to a lower biomass growth rate. However, to our knowledge, no study is currently available that clearly establishes the relative importance of oxygen availability and biomass quantity in OR-biocathode limitations.

So far, three different methods have been commonly described for designing OR-biocathodes. The first is based on the natural ability of biofilms to spontaneously develop on material surfaces. No polarization is applied to the electrode, the biofilm grows under open circuit conditions (OCP: open circuit potential), though it can subsequently demonstrate electrochemical activity when the biofilm-coated electrode is tested electrochemically [3–6]. Such biocathodes have notably been formed from seawater [5,6] and from laboratory cultures of single bacterial strains [3,4].

The second way of obtaining a biocathode is to polarize the electrode at a potential lower than the open circuit potential. The cathode polarization can result from MFC operation (potential may vary) [7–10] or from potentiostatic control (potential is constant) [11–18]. This method is widely used to form effective OR-biocathodes in many environments, among them sewage sludges or/and wastewater [8,13,15,18], industrial/agricultural wastes [7,9], seawater and sediments [14,17], soil and/or derived leachate [10–12].

Finally, following a procedure described by Cheng et al. [19], OR-biocathodes can be obtained by polarity reversion of already established bioanodes. Such reversible bioelectrodes are acetate-fed bioanodes that can be turned into OR-biocathodes after consecutive exhaustion of the acetate and supply of oxygen. The main advantage of this method is that a significant biomass can develop during the anodic phase. A practical benefit of reversible bioelectrodes used in MFCs is that they can be periodically reversed in order to neutralize acidification at the anode and alkalinizing at the cathode. The pH gradient formed between anode and cathode can thus be periodically neutralized, which helps to maintain the MFC performance during long-term operation [20,21].

Moreover, the biofilm acidification that occurs during the anode phase has been shown to favor the subsequent reduction of oxygen [22].

In this work, we report the comparison of OR-biocathodes designed using the three different methods: open circuit, conventional aerobic polarization, and polarization under reversible conditions, while all the other experimental parameters: electrolyte, inoculum, electrode material, reactor design, temperature and experiment timescale, are kept identical. OR-biocathodes are compared in terms of electrochemical performance, biofilm structure, and microbial community composition. Their electrochemical performances were evaluated using chronoamperometry (CA), OCP measurements and cyclic voltammetry (CV). The coverage of each OR-biocathode was imaged by scanning electron microscopy (SEM) and epifluorescence microscopy (EM). The microbial communities of the biofilms were analyzed after 16S-DNA gene pyrosequencing.

2. Experimental

2.1. Experimental medium: garden compost leachate

The garden compost leachate was prepared and filtered as described elsewhere [23]. It contained 20 mM of KCl in order to ensure medium conductivity ($5 \, mS \, cm^{-1}$). The initial pH of the leachate was around 7.8.

2.2. Biofilm designs: electrochemical set-ups and tests

Electrochemical experiments were performed with three-electrode setups in 650 mL of garden compost leachate. The electrodes and tubes for air supply were slipped through the cap holes of the Schott bottles that were used as electrochemical reactors. All the reactors had an open hole on the top in order to keep the solution in constant contact with air (quiescent conditions). The electrodes were: a 6 cm^2 piece of carbon cloth connected to a platinum wire as the working electrode, a saturated calomel electrode (SCE) as the reference electrode (248 mV/SHE) and a platinum grid as the counter-electrode. When indicated, air was supplied through a porous glass frit by means of an aquarium pump. A scheme of the electrochemical cells is available in supplementary data (Fig. SI 1).

The different experimental conditions for each electrochemical reactor are summarized in Table 1.

A potential of -0.2 V/SCE was applied to four electrodes (1 to 4), and two others were left at open circuit (5 and 6). In reactors 5 and 6, OCP was recorded throughout the experiment. Electrodes 1 and 2 were firstly fed by two pulses of 20 mM of sodium acetate to grow an anodic electroactive biofilm. This anodic phase was realized aerobically, the medium being in contact with ambient air. After substrate depletion, the bioanodes were reversed to oxygen reducing biocathodes by bubbling air into the reactors, as described in [22]. Electrodes 3 and 4 were polarized and no acetate was added, so that an oxygen-reducing cathodic biofilm developed spontaneously [11]. Periodically, CA (biocathodes 1–4) was interrupted for a rest period of 15 min before CVs were performed. CVs were performed at the same time for the biocathodes under open circuit (biocathodes 5 and 6). For CV analysis, the potential scan (1 mV s^{-1}) started from the OCP, went up to $+0.4$ V, down to -0.7 V/SCE and then back. All electrochemical tests were performed using a multichannel potentiostat (Biologic, France), with the EC-Lab software. Measurements of oxygen concentration were performed with an optical dissolved oxygen meter (WTW Multi 3410 purchased from WTW GmbH (Germany)). The oxygen concentration was $5.2 \pm 0.3 \, mg \, L^{-1}$ in the leachate under quiescent conditions and was brought to $6.7 \pm 0.2 \, mg \, L^{-1}$ during air supply.

2.3. Imaging: scanning electron microscopy and epifluorescence microscopy

At the end of the electrochemical experiments, electrodes were collected and divided in two parts, one for imaging and the other for population analyses. The parts destined for imaging were themselves cut in two, one part for scanning electron microscopy and the other for epifluorescence microscopy.

2.3.1. Scanning electron microscopy (SEM)

Biofilms were fixed using a solution of 4% glutaraldehyde in phosphate buffer (400 mM, pH = 7.4) and rinsed with a solution of saccharose (0.4 M) in phosphate buffer. Samples were then incubated for 1 h in phosphate buffer containing 2% of osmium tetroxide and saccharose. Finally, they were dehydrated by immersion in solutions containing increasing concentrations of acetone (from 50 to 100%), a mix of acetone and hexamethyldisilazane (HMDS) (50:50) and pure HMDS. After the last bath in HMDS, samples were dried until complete evaporation. SEM observations were made using a LEO 435 VP scanning electron microscope. Images were obtained using the SE1 detector, 200× magnification and a 10 kV electron beam.

2.3.2. Epifluorescence microscopy (EM)

Samples were stained with 0.03% acridine orange (A6014, Sigma) for 10 min, rinsed with sterile physiological water and then left to dry in the ambient air. Biofilms were imaged with a Carl Zeiss Axio Imager-M2 microscope equipped for epifluorescence with an HXP 200C light source and the Zeiss 09 filter (excitor HP450e 490, reflector FT 10, barrier filter LP520). Images were acquired with a digital camera (Zeiss AxioCam MRm) every 0.5 µm along the Z-axis and the set of images was processed with the Zen® software.

2.4. Microbial population analysis

Samples were sonicated in 2 mL of distilled water (2 × 3 min at a power level of 80 W, Fisher Scientific FB 15061) to suspend the biofilms. Biofilm suspensions were concentrated by centrifugation and finally resuspended in 500 µL of distilled water. The resulting 500 µL samples were kept at 3 °C before being sent to the Research and Testing Laboratory (RTLab – Lubbok, Texas, USA) for DNA extraction and microbial population analyses by 454 pyrosequencing (Roche). Primers used for the sequencing were 28F (5′-GAG TTT GAT YMT GGC TC-3′) and 519R (5′-GWA TTA CCG CGG CKG CTG-3′).

Data were screened and trimmed on the basis of quality scores; bases below a quality threshold of 25 were discarded. Sequences with less than 250 nt and chimeric sequences were removed using UCHIME [24,25]. Filtered sequences were further analyzed using the open source software QIIME [26] and clustered into operational taxonomic units (OTUs) at 97% sequence similarity using uclust [27]. Taxonomic assignment was performed down to the genus level by employing the RDP classifier with a 0.8 bootstrap cut-off, the most abundant sequence of an OTU being considered representative [28]. The Greengenes database

Table 1
Experimental conditions for electrode design.

Method	Biocathodes	Polarization	Acetate	Oxygen (mg L^{-1})	
				Quiescent	Air supply
Reversible polarization	1–2	-0.2 V/SCE	2 × 20 mM	5.2 ± 0.3	6.7 ± 0.2
Aerobic polarization	3–4	-0.2 V/SCE	No		
Open circuit condition	5–6	OCP	No		

(release gg_13_8_otus), included with the RDP classifier, was used for the taxonomic affiliations.

The diversity of the microbial population in each biofilm was assessed with the Shannon and Simpson diversity indices according to the number of operational taxonomic units (OTUs) following the equations:

$$\text{Shannon} = \frac{n_i}{\sum_{i=1}^{S} n_i} \times \ln\left(\frac{n_i}{\sum_{i=1}^{S} n_i}\right) \tag{1}$$

$$\text{Simpson} = \sum_{i=1}^{S} [n_i(n_i-1)]/[N(N-1)] \tag{2}$$

where n_i is the number of sequences belonging to the ith OTU and N is the total number of sequences remaining for the sample after quality control. S is the number of OTUs.

The heatmap of the normalized bacterial abundance at the order level and the corresponding hierarchical clustering were obtained with the QIIME software. The distance matrix was built up using the Bray-Curtis method and the hierarchical clustering was performed with the average linkage method.

3. Results

3.1. Electrochemical characterization

3.1.1. Reversible OR-biocathodes

Chronoamperometries recorded with reversible bioelectrodes are presented in Fig. 1.

Two additions of acetate were performed, which led to two oxidation peaks (Fig. 1A). The current densities reached 9.0 ± 1.0 and 15.8 ± 0.6 A m^{-2} following the two acetate additions. These values were in accordance with previous works on the formation of bioanodes from compost leachate [23,29].

At 19.9 days, when the current of acetate oxidation was almost negligible, air was supplied to the electrochemical cells for 24 h to reverse the acetate-oxidizing bioanodes into OR-biocathodes. Current densities immediately dropped, down to -0.17 ± 0.02 A m^{-2} and reached around -0.05 ± 0.01 A m^{-2} after 24 h. When forced aeration was stopped, current densities immediately became close to zero in both reactors, even returning to an oxidative value for electrode 2 (around 0.01 A m^{-2}). This can be explained by the persistence of a small acetate residue. A complete exhaustion of the substrate is indeed necessary for a definitive conversion of the electrode into biocathode, otherwise a persistent oxidative current for acetate oxidation opposed to the lower OR-cathodic current. A second 24 h period of forced aeration was performed after 24 h in order to definitely convert the bioanodes to OR-biocathodes. Reductive current densities instantly reached -0.10 ± 0.01 A m^{-2} and -0.05 ± 0.02 A m^{-2} after 24 h of aeration.

3.1.2. Biocathodes designed using aerobic polarization

CAs for the same 23 days, recorded with OR-biocathodes under constant aerobic polarization at -0.2 V/SCE (electrodes 3–4), are displayed in Fig. 2.

Current densities for oxygen reduction started to be observed after half a day of polarization, and quickly stabilized around -0.02 A m^{-2} after 1.5 days. They remained stable for the four following days and then dropped again around day 5.5. They stabilized around -0.19 ± 0.01 and -0.27 ± 0.12 A m^{-2} after ten days, with a minimal value at -0.39 A m^{-2} (electrode 4, day 13.8). Forced aeration at 19.9 days caused a brief fall in the current density (down to -0.77 A m^{-2} with electrode 4), followed by a fast increase. Current densities finally stabilized around -0.035 ± 0.005 A m^{-2} after 12 h of forced aeration, returning to values initially observed before 5.2 days.
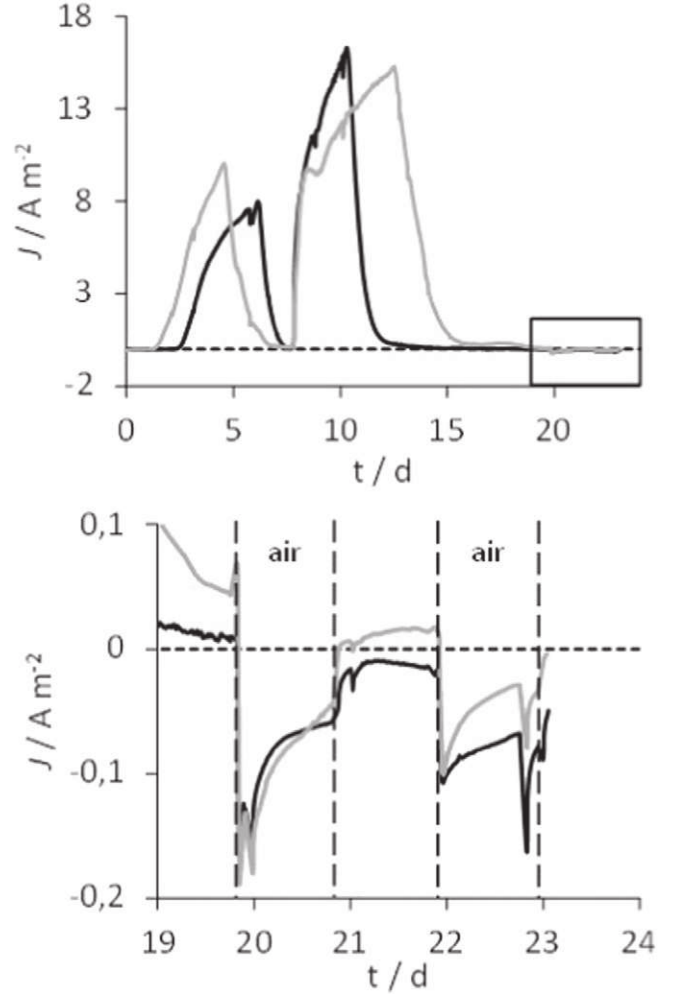
Fig. 1. Chronoamperometries recorded with reversible bioelectrodes 1 (black line) and 2 (grey line). Panel A shows the whole CA, with the anodic phase consisting of 2 cycles of acetate oxidation (20 mM). The inset expanded in panel B displays the cathodic phase during the last five days. During this phase, forced aeration was supplied to the electrochemical reactor for two periods of 24 h separated by 24 h. Other current peaks at days 20, 21 and 22.8 were due to CV recording.
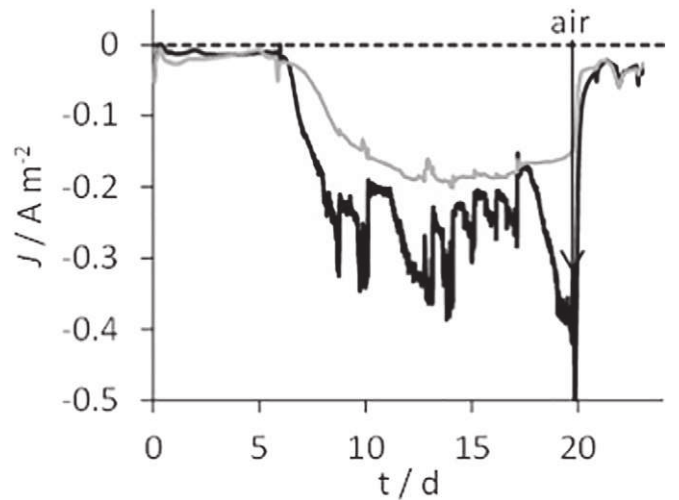
Fig. 2. CA recorded for polarized OR-biocathodes 3 (black line) and 4 (grey line) without acetate addition. Both were formed under constant polarization at -0.2 V/SCE. Air was forced into the electrochemical reactors at 19.9 days, bringing the oxygen concentration up from 5.2 ± 0.3 to 6.7 ± 0.2 mg L^{-1}.

3.1.3. Biocathodes formed at open circuit

The variations of OCP with time, recorded when forming OR-biocathodes 5 and 6, are presented in the supplementary information (Fig. SI 2). OCPs were initially 139 and 197 mV/SCE respectively for electrodes 5 and 6. They rose to 306 and 361 mV after 4 days. This potential increase, well known in microbial corrosion, corresponded to the initial establishment of a cathodic biofilm on the electrode [30]; it could be related to the lag time observed before current generation in the case of electrodes formed under polarization. Except for punctual drops after cyclic voltammetry recordings at 5.9, 9.8 and 12.8 days, OCP values remained stable throughout the experiment, at mean values of 275 ± 4 (electrode 5) and 385 ± 5 mV (electrode 6). Forced aeration on day 19.9 caused an immediate drop, down to 170 and 260 mV for electrodes 5 and 6 respectively.

3.1.4. Voltammetric analysis

Two distinct reduction waves, numbered I and II were observed on the voltammetric curves depending on the aeration (Fig. 3). Wave I was observed around -0.30 V/SCE with reversible electrodes (Fig. 3A) and electrodes formed at OCP (Fig. 3C). It was also observed with OR-biocathodes formed under aerobic polarization, but only after exposure to forced aeration (at 19.9 days) (Fig. 3B). Wave II was observed around $+0.23$ V/SCE, with these electrodes only, prior to forced aeration. As established recently, waves I and II are the electrochemical signatures of two distinct biological redox systems catalyzing the OR [12]. On CA (Fig. 1), system I was responsible for the current production observed with reversible bioelectrodes whereas system II was responsible for the lower current densities observed with aerobically polarized biocathodes before exposure to forced aeration.

3.2. Biofilm structures

Three different electrode coverages were evidenced depending on the method used to form the OR-biocathodes. The highest colonization was obtained with the reversible biocathode: both epifluorescence and SEM revealed complete coverage of the carbon cloth surface, with square patches of biofilm on the carbon cloth mesh that made individual carbon fibers hardly distinguishable (Fig. 4A).The biocathodes formed at OCP (Fig. 4C) remained poorly colonized compared to the polarized ones. No biofilm was visible by SEM (Fig. 4C1) and practically no colonization was detected by epifluorescence (Fig. 4C2). Images of the OR-biocathodes formed under aerobic polarization (Fig. 4B) revealed a degree of colonization between those of biocathodes formed on OCP and reversible biocathodes.

3.3. Population analyses

3.3.1. Statistics

After trimming and sorting, DNA sequences were clustered into 1689 different OTUs. The number of OTUs identified for each electrode, together with the corresponding Shannon and Simpson diversity indices, are presented in Table 2.

The diversity indices indicated a rather high diversity on the electrodes. Simpson indices were high, ranging from 0.807 to 0.952, demonstrating that the biofilms were not dominated by a few OTUs. The reversible bioelectrodes (1 and 2) displayed the lowest richness in represented OTUs (265 and 428 respectively), the lowest diversity (Shannon indices 3.83 and 4.31) and tended to be more dominated by single OTUs than the others (lower Simpson indices, 0.807 and 0.808). The Shannon and Simpson indices in Table 1 did not permit populations from aerobically polarized (3 and 4) and OCP electrodes (5 and 6) to be unambiguously distinguished.

3.3.2. Major genera

Major genera and their corresponding taxonomic affiliations represented in each biofilm are given in Table 3.
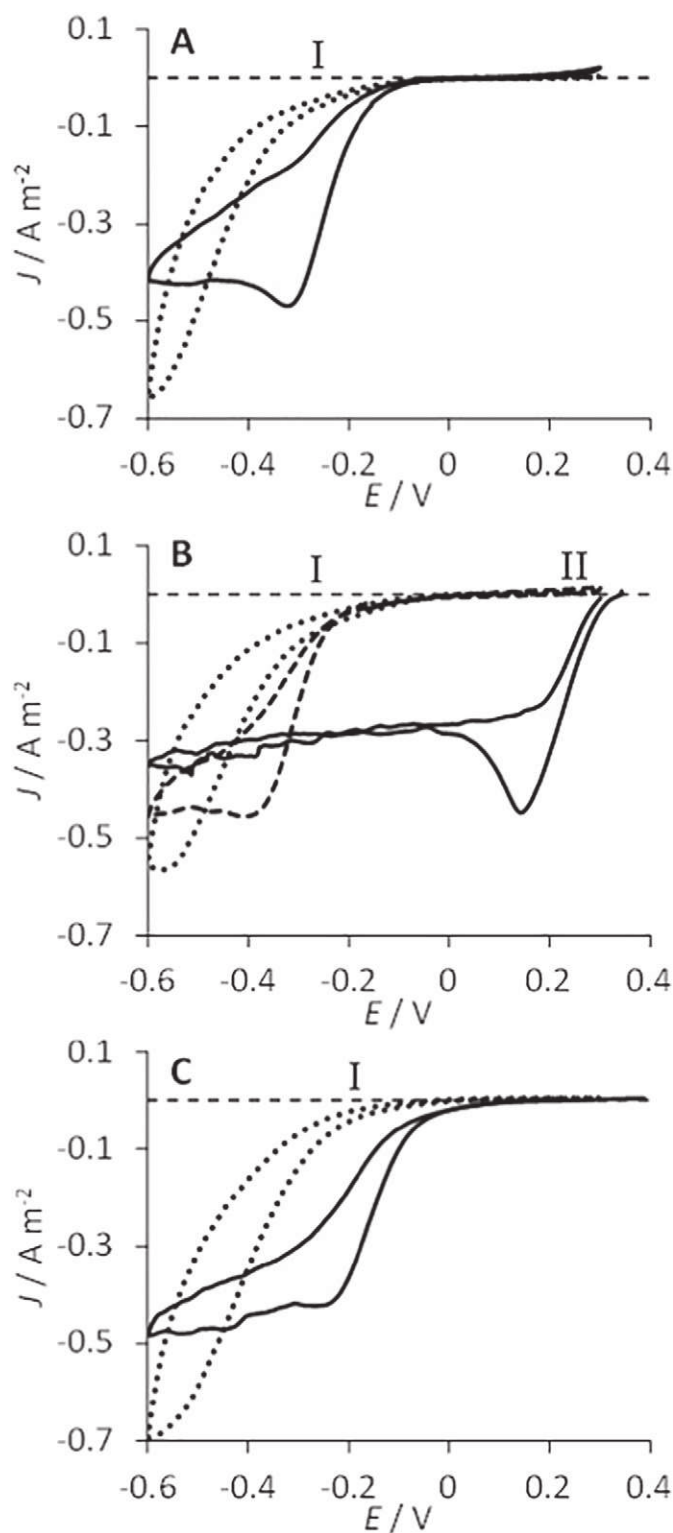
Fig. 3. Representative cyclic voltammograms recorded with the three types of OR-biocathodes. A: reversible bioelectrode, B: Aerobically polarized OR-biocathode, C: OR-biocathode formed at OCP. Dotted line: control ($t = 0$); solid line: before forced aeration (after 19.9 days); dashed line: immediately after forced aeration was stopped. The voltammograms recorded after forced aeration was stopped were identical to the ones recorded before with reversible bioelectrodes (A) and bioelectrodes formed at OCP (C) (and not presented). All voltammograms were recorded under quiescent conditions (i.e. the forced aeration was stopped).

In accordance with the diversity indices, communities on reversible electrodes tended to be more dominated by a single genus ($41.1 \pm 1.3\%$ for the dominant genus) than communities on the aerobically polarized
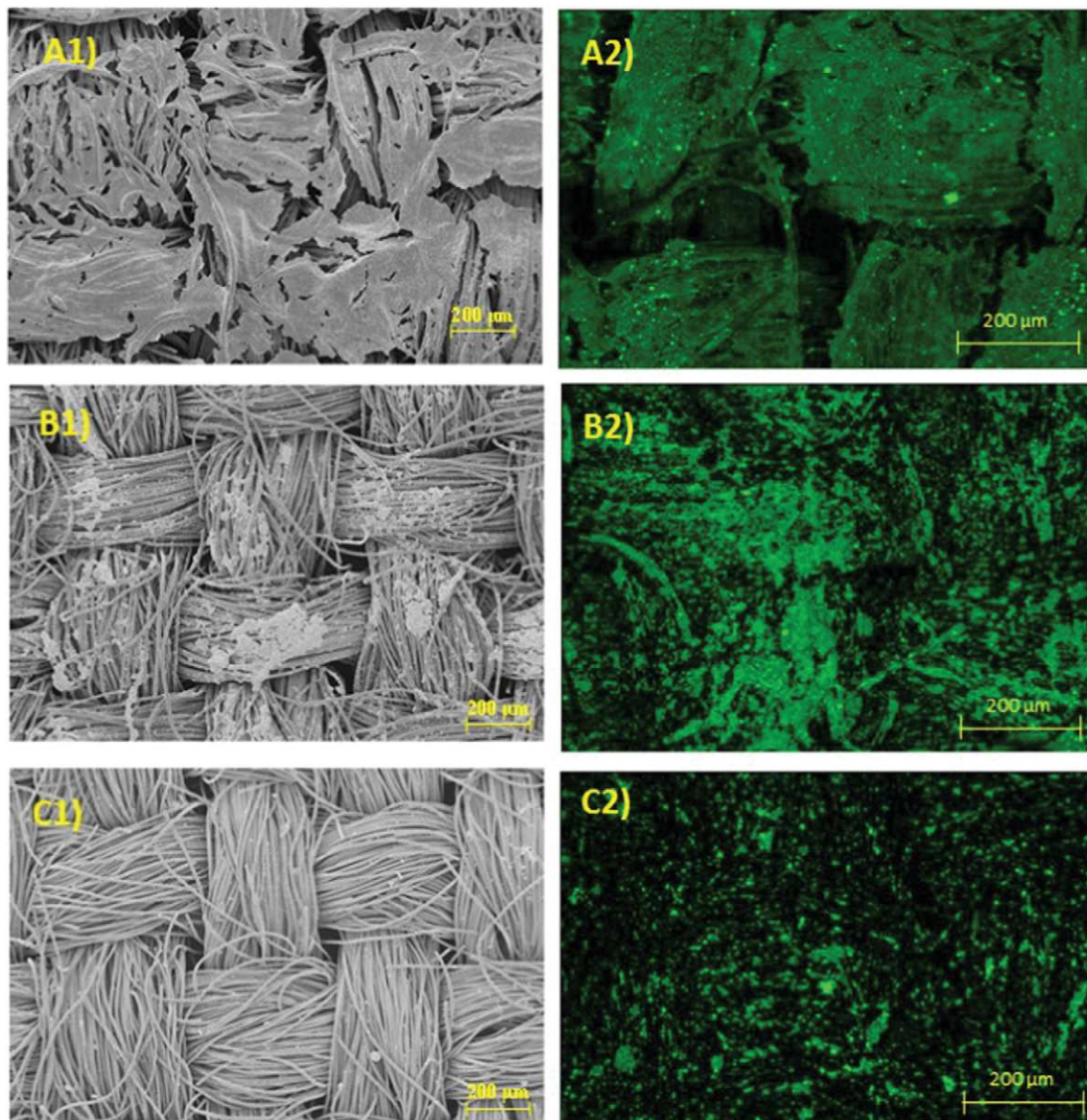
Fig. 4. Images of biofilms obtained by SEM (A1, B1 and C1) and epifluorescence microscopy (A2, B2, C2) respectively developed on reversible (A), aerobically polarized (B) and OCP OR (C) biocathodes.

(30.8 ± 6.0%) and OCP biocathodes (20.2 ± 3.7%). *Arenimonas* (Gammaproteobacteria) were found to be dominant on electrode 1 (39.8%), followed by the genus *Pseudomonas* (13.5%) and another unidentified genus from the Xanthomonadaceae family (11.8%) (both belonging to Gammaproteobacteria). Sequences attributed to the genus *Chryseobacterium* (Bacteroidetes) were found to be dominant on electrode 2 (42.5%), followed by the same unidentified Xanthomonadaceae (8.8%) also present on electrode 1.

Table 2
Number of OTUs identified, with Shannon and Simpson diversity indices calculated for each electrode.

Electrodes	Observed OTUs	Shannon	Simpson
1	265	3.83	0.807
2	428	4.31	0.808
3	530	6.29	0.951
4	501	5.01	0.868
5	515	6.61	0.952
6	478	5.69	0.930

Communities on biocathodes formed under aerobic polarization and open circuit conditions were dominated by the same genus, *Sporosarcina* (Firmicutes). Sequences attributed to this genus scored between 36.8 and 16.6% of all the sequences on electrodes 4 and 6 respectively. *Brevundimonas* (Alphaproteobacteria) was found as a common second dominant on aerobically polarized biocathodes (11.9% and 21.9% on electrodes 3 and 4). The genus *Chryseobacterium*, also identified on electrode 2, was co-dominant with *Sporosarcina* (16.6%) on electrode 6 and *Pseudomonas* ranked second on electrode 5 (10.9%).

4. Discussion

4.1. Electrode performances

The range of steady state current densities (-0.05 ± 0.02 and -0.27 ± 0.12 A m^{-2} at -0.2 V/SCE) achieved here by the reversible and aerobically polarized OR-biocathodes were consistent with values already reported in the literature for such biocathodes formed from compost leachate inoculum [11,12,22]. Biocathodes formed under aerobic polarization displayed higher current densities (electrodes 3–4)

Table 3
Proportion and taxonomic affiliation of major bacterial genera identified in the six biofilms (at least 2% of the whole bacterial population on at least one electrode).
Only genera representing more than 2% of the community present in at least one biofilm are presented. Other genera are grouped in the "other" category. The proportions of the five dominant genera in each biofilm are highlighted in graded shades of red.

Phylum	Class	Order	Family	Genus	1	2	3	4	5	6
Acidobacteria	iii1-8	DS-18	Unidentified	Unidentified	0.0	0.0	20	0.9	3.2	1.6
Bacteroidetes	Cytophagia	Cytophagales	Cytophagaceae	*Hymenobacter*	0.0	0.0	0.0	6.9	0.0	0.0
Bacteroidetes	Flavobacteriia	Flavobacteriales	Weeksellaceae	*Chryseobacterium*	10.8	42.5	0.0	0.0	0.0	16.6
Bacteroidetes	Flavobacteriia	Flavobacteriales	Weeksellaceae	Other	1.7	3.8	0.0	0.0	0.0	2.1
Bacteroidetes	Rhodothermi	Rhodothermales	Balneolaceae	Unidentified	0.0	3.4	0.0	0.0	0.0	0.0
Bacteroidetes	Saprospirae	Saprospirales	Chitinophagaceae	Unidentified	0.0	0.1	2.4	5.6	2.0	0.5
Bacteroidetes	Saprospirae	Saprospirales	Saprospiraceae	Unidentified	0.0	0.0	0.1	0.3	3.5	0.2
Chloroflexi	Anaerolineae	envOPS12	Unidentified	Unidentified	0.1	5.1	0.2	0.2	0.1	0.0
Chloroflexi	Anaerolineae	GCA004	Unidentified	Unidentified	3.0	0.2	1.9	0.6	0.1	1.0
Firmicutes	Bacilli	Bacillales	Planococcaceae	*Sporosarcina*	0.5	0.4	24.8	36.8	23.9	16.6
Planctomycetes	Phycisphaerae	Phycisphaerales	Unidentified	Unidentified	0.0	4.5	0.7	0.1	0.5	0.1
Proteobacteria	Alpha-	Caulobacterales	Caulobacteraceae	*Brevundimonas*	0.0	0.0	11.9	21.9	0.7	1.4
Proteobacteria	Alpha-	Other	Other	Other	0.1	0.4	2.5	2.2	3.7	1.2
Proteobacteria	Alpha-	Rhizobiales	Hyphomicrobiaceae	*Parvibaculum*	0.0	0.1	2.3	0.5	0.6	0.3
Proteobacteria	Alpha-	Rhizobiales	Hyphomicrobiaceae	Unidentified	0.1	0.1	3.0	0.8	2.5	0.5
Proteobacteria	Alpha-	Rhodospirillales	Rhodospirillaceae	Phaeospirillum	0.1	0.0	3.8	0.3	1.6	4.7
Proteobacteria	Alpha-	Rhodospirillales	Rhodospirillaceae	Unidentified	0.5	1.2	3.6	0.3	0.7	1.7
Proteobacteria	Beta-	Burkholderiales	Comamonadaceae	*Delftia*	0.0	0.0	0.0	0.0	0.0	13.9
Proteobacteria	Beta-	Burkholderiales	Comamonadaceae	*Hydrogenophaga*	0.4	0.0	3.0	0.3	0.3	1.1
Proteobacteria	Beta-	Rhodocyclales	Rhodocyclaceae	Unidentified	4.0	0.0	0.0	0.0	0.1	0.0
Proteobacteria	Gamma-	Chromatiales	Unidentified	Unidentified	2.7	0.7	0.1	0.0	0.1	0.1
Proteobacteria	Gamma-	Other	Other	Other	0.5	0.3	8.9	1.6	0.2	0.5
Proteobacteria	Gamma-	Pseudomonadales	Pseudomonadaceae	*Pseudomonas*	13.5	0.1	1.2	0.3	10.9	1.1
Proteobacteria	Gamma-	Xanthomonadales	Sinobacteraceae	Other	0.0	3.0	0.0	0.0	0.0	0.0
Proteobacteria	Gamma-	Xanthomonadales	Xanthomonadaceae	*Arenimonas*	39.8	6.9	0.1	0.0	3.8	0.1
Proteobacteria	Gamma-	Xanthomonadales	Xanthomonadaceae	Other	11.8	8.8	0.1	0.1	0.2	0.2
Proteobacteria	Gamma-	Xanthomonadales	Xanthomonadaceae	*Stenotrophomonas*	0.2	0.0	0.3	0.0	0.0	10.3
Other	Other	Other	Other	Other	10.3	18.4	27.1	20.4	41.3	24.3

than reversible ones (electrodes 1–2), due to the two different electrochemical systems involved in the electron transfer from the electrode to oxygen. System I corresponded to a bacterial redox system responsible for a direct electron transfer with the electrode, possibly a membrane-bound cytochrome. System II corresponded to an oxygen reduction mechanism based on a soluble redox mediator that was highly sensitive to the hydrodynamic stress created by forced aeration [12]. Agitation of the bulk solution caused the dispersion of the soluble mediator outside the biofilm. The fact that the procedure to turn reversible bioelectrodes into OR-biocathodes relies on forced aeration explains why no electrochemical signal relating to system II was observed with electrodes 1 and 2. Additional experiments performed without forced aeration to activate the reversion of the bioanode into OR-Biocathode revealed that system II started to be observed around 10 days after the end of the last cycle of acetate consumption (data not shown).

CVs recorded with biocathodes formed at OCP revealed an oxygen reduction related to system I only. The evolution of OCP values measured with these electrodes was intriguing, however. They evolved from +330 mV/SCE (on average for the two reactors) before to +215 mV/SCE after forced aeration at 19.9 days. The OCP value is the result of the balance between the cathodic (mainly oxygen reduction in aerobic conditions) and anodic (e.g. oxidation of surface compounds) reactions occurring spontaneously on the electrode surface. This is the

principle of the redox sensors used to assess the aerobic/anaerobic level of media, for instance. OCP is consequently expected to increase when the cathodic reactions are enhanced by aeration. Here, the opposite was observed. Under open circuit conditions, the reactions that could spontaneously occur on the electrode surface were very slow and possibly sensitive to any small modification of the operating conditions. Thus, the high OCP values observed before aeration might be explained by possible traces of system II that were too small to be detected by voltammetry. Indeed, the estimated potential of system II, +0.23 V, fell within this potential range. The OCP decrease would be explained by the forced aeration which drove away the traces of system II.

The electrochemical results confirmed the ubiquity of redox system I, which was observed as a basal OR-system whatever the method used to form the OR-biocathodes. They also demonstrated the necessity to polarize the electrode in order to induce the significant occurrence of redox system II.

4.2. Electrode coverages by microbial biofilms

Both the quantity of biofilm and the coverage of the carbon cloth by the biofilm was clearly higher on the reversible electrodes than on the others. The presence of substrate (acetate) during the anodic phase sustained the bacterial proliferation [32]. This strategy was successfully

exploited by researchers aiming to obtain reversible bioelectrodes with an increased amount of biomass for enhanced CO_2 reduction [33].

The higher coverage on the polarized electrodes (both reversible and aerobically polarized biocathodes) compared to biocathodes formed at OCP may indicate that some bacteria were capable of autotrophic growth using the polarized electrode as an electron source [33–35].

There was no correlation between electrochemical performance and biomass accumulated on the electrodes. A similar peak current density $(0.45 \pm 0.02$ A m$^{-2})$ was observed by CV under quiescent conditions with both the poorly colonized OC-formed biocathodes and the massively covered reversible bioelectrodes. This is characteristic of a limitation of OR-catalysis by the availability of dissolved oxygen [36]. It reflects both the efficiency of the catalyst in the case of the thinly colonized, OCP-formed biocathodes and the efficient oxygen or electron transfer through the biofilm in the case of reversible bioelectrodes. Low oxygen availability thus seemed to be a more stringent limitation than the low biomass developed on some electrodes, at least in the aeration condition/quiescent conditions tested here.

4.3. Performance and microbial communities

4.3.1. Comparison between the different electrodes

A heatmap of the normalized abundances of the various bacterial orders was drawn to assess the ecological distance between the different biocathodes (Fig. 5).

The hierarchical clustering (top of the heatmap) showed two different clusters at the highest distance level. One cluster was formed by the populations identified on reversible electrodes (1 and 2) and the other contained the populations identified on the other four electrodes (3 to 6). Bacteroidetes and Gammaproteobacteria were present in large numbers in the biofilms from the reversible electrodes (1 and 2), while Firmicutes and Proteobacteria from the alpha- and beta- classes dominated in the biofilms from the other electrodes (3 to 6). Chae et al. demonstrated that feeding bioanodes with different substrates to oxidize led to the selection of different microbial populations inside the biofilms [37]. The addition of acetate as a substrate during the formation of the reversible biocathodes would have played a crucial role in selecting

populations different from those on the other, unfed, electrodes. This higher selection on such electrodes was confirmed by their lower Shannon and Simpson indices, which indicated the development of biofilms more dominated by single species.

Populations from biocathodes formed under aerobic polarization and open circuit conditions were clustered together in the heatmap and thus could not be differentiated in this way. They showed close values of Shannon and Simpson indices and had *Sporosarcina* as a common dominant genus. A distinctive feature, however, that clearly differentiated the communities from these electrodes was the selection of Caulobacterales, especially genus *Brevundimonas,* on polarized biocathodes, where it was second dominant, whereas it was minor on electrodes formed at OCP. This selection has to be linked to the applied potential, -0.2 V/SCE. A lower selection occurred when no potential was applied, as reflected by the fairly equal proportions of the dominant communities identified on the OCP-formed biocathodes (5–6). The common presence of *Sporosarcina* on biocathodes 3 to 6 could be explained by a high proportion of *Sporosarcina* in the starting inoculum, which would have led to its easy enrichment inside the four biofilms. On the other hand, *Brevundimonas*, though likely a minor component of the inoculum (low presence on electrodes 5 and 6), may have profited from the electrode potential to proliferate on aerobically polarized biocathodes (3–4), but not on the electrodes formed at OCP (5–6).

As the genus dominant exclusively on biocathodes formed under aerobic polarization, *Brevundimonas* may be a good candidate to provide redox system II, which was detected only on these electrodes. This genus is phylogenetically closely related to the genus *Caulobacter* [38]. These bacteria are known to be able to grow on media with a low organic matter content, as was the case with OR-biocathodes in compost leachate. Some of them produce prosthecae (cellular excrescences), which may play a role in electron exchange with the electrode. Some *Brevundimonas* such as *Brevundimonas lenta* [39] and *Brevundimonas terrae* [40] are known to produce Q10 and Q8 derived quinones that would fit perfectly with the soluble mediator nature of redox system II described in [12]. Redox system I, on the other hand, was detected on the six electrodes and so could not be linked to the presence of a particular genus of bacteria. As detailed in [12], this system ensured a basal
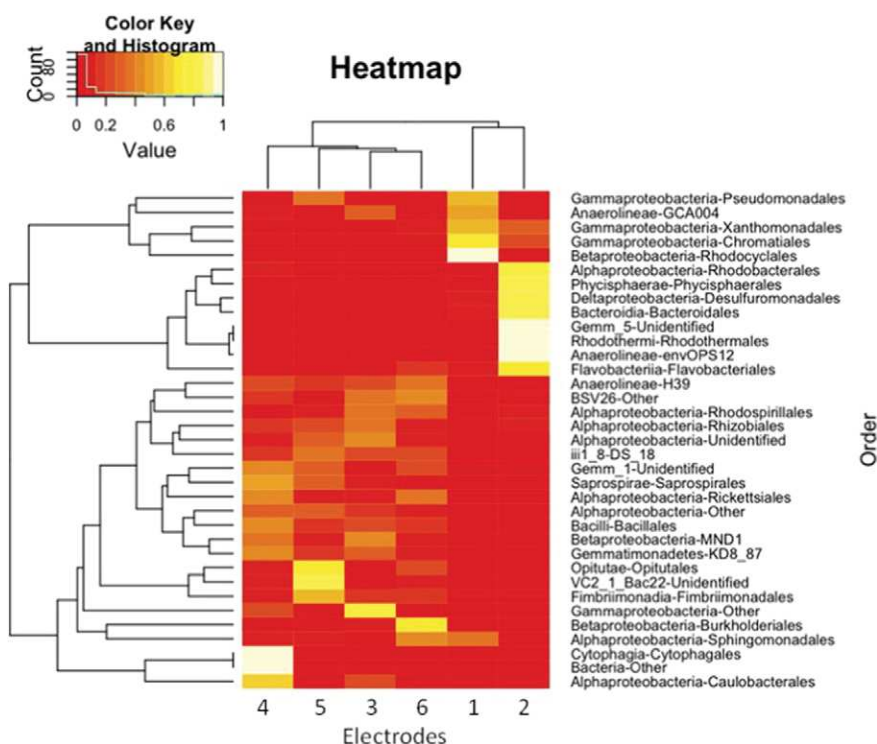

Fig. 5. Heatmap of the normalized bacterial abundance at the order level (filter at 1% of abundance on at least 1 of the 6 electrodes) and hierarchical clustering.

electrochemical activity and was ubiquitously detected in electroactive biofilms designed using different inocula, different electrode materials and different methods. This study further highlighted these characteristics.

4.3.2. Comparison with the literature

Populations detected on reversible OR-biocathodes differed from populations identified in the literature by Blanchet et al., who observed a dominance ($49 \pm 1\%$) of the phylum Chloroflexi (genera *Chloroflexus*, *Longilinea*, *Bellilinea* and *Anaerolinea*) [22]. When this specific phylum was disregarded, however, proportions of Proteobacteria, Firmicutes and Bacteroidetes in their biofilms were similar to those observed here. In these phyla, they identified the genera *Azoarcus*, *Thauera* (Betaproteobacteria), *Bacillus* (Firmicutes) and *Balneola* (Bacteroidetes) as dominant. *Sporosarcina* spp. and *Chryseobacterium* spp. were detected, but in a lower proportion. Due to the aerobic/oxic conditions, bacteria from the order Desulfuromonadales (Geobacteraceae) were not enriched, even if the electrodes were firstly fed with acetate during the anodic phase. This distinguished the populations originating from reversible bioelectrodes from those found on anaerobic bioanodes [23].

Dominant genera on aerobically polarized OR-biocathodes belonged to order Bacillales (Firmicutes), Caulobacterales and Rhizobiales (Alphaproteobacteria). Some Bacillales have previously been found on OR-biocathodes and have been proven to be electroactive [4,41,42]. A similar association of Bacilli and Alphaproteobacteria was observed by Desmond-Le Quéméner et al. for OR-biocathodes formed from a similar inoculum but polarized at a lower potential, -0.4 V/SCE [11]. These electrodes displayed lower current densities than the aerobically polarized biocathodes described here, as redox system II was not detected in these biofilms, probably due to the low polarization potential (-0.4 V/SCE). In the same work, however, electrodes polarized at a higher potential ($+0.1$ V/SCE) demonstrated similar performance, with a development of redox system II. But the communities on these last mentioned biocathodes were strongly dominated by Gammaproteobacteria, which have been found to dominate communities on efficient OR-biocathodes in several studies [15–18]. All the differences pointed out here can be linked to the different potentials used to polarize the electrodes, -0.4, -0.2 and $+0.1$ V/SCE, which conditioned the bacterial selection and the development of an efficient redox system for oxygen reduction (redox system II).

5. Conclusions

The three methods used to form OR-biocathodes led to the formation of similarly aged electrodes displaying different electrochemical performances, different electrode coverage and different bacterial communities. Biocathodes formed under polarization in aerobic conditions reduced oxygen at $+0.23$ V/SCE (redox system II) and thus demonstrated the best electrochemical performance at -0.2 V/SCE. Due to the procedure used to form them, reversible bioelectrodes displayed the highest electrode coverage by the biofilm and a distinctive selection of bacterial populations. The study emphasizes the importance of the polarization in obtaining denser biofilms (reversible and aerobic biocathodes versus biocathodes formed at open circuit), a higher selection of bacterial species (aerobically polarized versus OCP-formed biocathodes) and higher electrochemical performance (development of redox system II on aerobically polarized biocathodes). This work also highlights the different behavior of the two redox systems identified. System I was found in all biofilms, whatever the procedure used to achieve the electrode and the bacterial population. It is confirmed as a recurring signature of oxygen-reducing electroactive biofilms. System II was evidenced only in biofilms grown under polarization and not exposed to hydrodynamic stress such as forced aeration. Its higher redox potential ($+0.23$ V/SCE) is of great interest for MFC applications, but appropriate implementation conditions will be necessary because of its sensitivity to hydrodynamic conditions. Moreover, the bacterial

genera responsible for system II remain to be determined and the extensive comparison of microbial populations made here indicates *Brevundimonas* spp. as a possibly essential genus from this point of view. Checking *Brevundimonas* spp. would be a very interesting, innovative way of pursuing the objective of designing system-II-based OR-biocathodes. Lastly, this study demonstrates that oxygen availability, rather than the biomass on the electrode surface, was the main limiting factor in the improvement of OR-biocathodes, at least with the aeration conditions experienced here. Future studies will have to elaborate procedures in which more oxygen will be brought to the biofilm without increasing hydrodynamic stresses, which are detrimental to redox system II. In this context, the ongoing development of micro-fluidics studies and devices will be of great interest in the future of MFCs.

Supplementary data to this article can be found online at http://dx.doi.org/10.1016/j.bioelechem.2017.03.001.

References

[1] B. Erable, D. Feron, A. Bergel, Microbial catalysis of the oxygen reduction reaction for microbial fuel cells: a review, Chemsuschem 5 (2012) 975–987, http://dx.doi.org/10.1002/cssc.201100836.

[2] L. Huang, J.M. Regan, X. Quan, Electron transfer mechanisms, new applications, and performance of biocathode microbial fuel cells, Bioresour. Technol. 102 (2011) 316–323.

[3] A. Cournet, M. Berge, C. Roques, A. Bergel, M.-L. Delia, Electrochemical reduction of oxygen catalyzed by Pseudomonas aeruginosa, Electrochim. Acta 55 (2010) 4902–4908, http://dx.doi.org/10.1016/j.electacta.2010.03.085.

[4] A. Cournet, M.-L. Delia, A. Bergel, C. Roques, M. Berge, Electrochemical reduction of oxygen catalyzed by a wide range of bacteria including gram-positive, Electrochem. Commun. 12 (2010) 505–508, http://dx.doi.org/10.1016/j.elecom.2010.01.026.

[5] B. Erable, I. Vandecandelaere, M. Faimali, M.-L. Delia, L. Etcheverry, P. Vandamme, A. Bergel, Marine aerobic biofilm as biocathode catalyst, Bioelectrochemistry 78 (2010) 51–56, http://dx.doi.org/10.1016/j.bioelechem.2009.06.006.

[6] F. Xu, J. Duan, B. Hou, Electron transfer process from marine biofilms to graphite electrodes in seawater, Fundam. Microb. Power Plants Electrochem. Act. Biofilms 78 (2010) 92–95, http://dx.doi.org/10.1016/j.bioelechem.2009.09.010.

[7] Z. Wang, T. Lee, B. Lim, C. Choi, J. Park, Microbial community structures differentiated in a single-chamber air-cathode microbial fuel cell fueled with rice straw hydrolysate, Biotechnol. Biofuels 7 (2014) 9, http://dx.doi.org/10.1186/1754-6834-7-9.

[8] P. Cristiani, M.L. Carvalho, E. Guerrini, M. Daghio, C. Santoro, B. Li, Cathodic and anodic biofilms in single chamber microbial fuel cells, Bioelectrochemistry 92 (2013) 6–13, http://dx.doi.org/10.1016/j.bioelechem.2013.01.005.

[9] G. Zhang, Q. Zhao, Y. Jiao, K. Wang, D.-J. Lee, N. Ren, Biocathode microbial fuel cell for efficient electricity recovery from dairy manure, Biosens. Bioelectron. 31 (2012) 537–543.

[10] Z. Chen, Y. Huang, J. Liang, F. Zhao, Y. Zhu, A novel sediment microbial fuel cell with a biocathode in the rice rhizosphere, Bioresour. Technol. 108 (2012) 55–59, http://dx.doi.org/10.1016/j.biortech.2011.10.040.

[11] E. Desmond-Le Quéméner, M. Rimboud, A. Bridier, C. Madigou, B. Erable, A. Bergel, T. Bouchez, Biocathodes reducing oxygen at high potential select biofilms dominated by ectothiorhodospiraceae populations harboring a specific association of genes, Bioresour. Technol. 214 (2016) 55–62, http://dx.doi.org/10.1016/j.biortech.2016.04.087.

[12] M. Rimboud, A. Bergel, B. Erable, Multiple electron transfer systems in oxygen reducing biocathodes revealed by different conditions of aeration/agitation, Bioelectrochemistry 110 (2016) 46–51, http://dx.doi.org/10.1016/j.bioelechem.2016.03.002.

[13] M. Rimboud, E. Desmond-Le Quemener, B. Erable, T. Bouchez, A. Bergel, The current provided by oxygen-reducing microbial cathodes is related to the composition of their bacterial community, Bioelectrochemistry 102 (2015) 42–49, http://dx.doi.org/10.1016/j.bioelechem.2014.11.006.

[14] S. Debuy, S. Pecastaings, A. Bergel, B. Erable, Oxygen-reducing biocathodes designed with pure cultures of microbial strains isolated from seawater biofilms, Int. Biodeterior. Biodegrad. 103 (2015) 16–22, http://dx.doi.org/10.1016/j.ibiod.2015.03.028.

[15] M. Rothballer, M. Picot, T. Sieper, J.B.A. Arends, M. Schmid, A. Hartmann, N. Boon, C.J.N. Buisman, F. Barriere, D.P.B.T.B. Strik, Monophyletic group of unclassified gamma-Proteobacteria dominates in mixed culture biofilm of high-performing oxygen reducing biocathode, Bioelectrochemistry 106 (2015) 167–176, http://dx.doi.org/10.1016/j.bioelechem.2015.04.004.

[16] E. Milner, K. Scott, I. Head, T. Curtis, E. Yu, Electrochemical investigation of aerobic biocathodes at different poised potentials: evidence for mediated extracellular electron transfer, Chem. Eng. Trans. 41 (2014) 355, http://dx.doi.org/10.3303/CET1441060.

[17] S.M. Strycharz-Glaven, R.H. Glaven, Z. Wang, J. Zhou, G.J. Vora, L.M. Tender, Electrochemical investigation of a microbial solar cell reveals a Nonphotosynthetic biocathode catalyst, Appl. Environ. Microbiol. 79 (2013) 3933–3942, http://dx.doi.org/10.1128/AEM.00431-13.

[18] X. Xia, Y. Sun, P. Liang, X. Huang, Long-term effect of set potential on biocathodes in microbial fuel cells: electrochemical and phylogenetic characterization, Bioresour. Technol. 120 (2012) 26–33, http://dx.doi.org/10.1016/j.biortech.2012.06.017.

[19] K.Y. Cheng, G. Ho, R. Cord-Ruwisch, Anodophilic biofilm catalyzes cathodic oxygen reduction, Environ. Sci. Technol. 44 (2010) 518–525, http://dx.doi.org/10.1021/es9023833.

[20] W. Li, J. Sun, Y. Hu, Y. Zhang, F. Deng, J. Chen, Simultaneous pH self-neutralization and bioelectricity generation in a dual bioelectrode microbial fuel cell under periodic reversion of polarity, J. Power Sources 268 (2014) 287–293, http://dx.doi.org/10.1016/j.jpowsour.2014.06.047.

[21] D.P.B.T.B. Strik, H.V.M. Hamelers, C.J.N. Buisman, Solar energy powered microbial fuel cell with a reversible bioelectrode, Environ. Sci. Technol. 44 (2010) 532–537, http://dx.doi.org/10.1021/es902435v.

[22] E. Blanchet, S. Pécastaings, B. Erable, C. Roques, A. Bergel, Protons accumulation during anodic phase turned to advantage for oxygen reduction during cathodic phase in reversible bioelectrodes, Bioresour. Technol. 173 (2014) 224–230, http://dx.doi.org/10.1016/j.biortech.2014.09.076.

[23] B. Cercado, N. Byrne, M. Bertrand, D. Pocaznoi, M. Rimboud, W. Achouak, A. Bergel, Garden compost inoculum leads to microbial bioanodes with potential-independent characteristics, Bioresour. Technol. 134 (2013) 276–284.

[24] S.E. Dowd, T.R. Callaway, R.D. Wolcott, Y. Sun, T. McKeehan, R.G. Hagevoort, T.S. Edrington, Evaluation of the bacterial diversity in the feces of cattle using 16S rDNA bacterial tag-encoded FLX amplicon pyrosequencing (bTEFAP), BMC Microbiol. 8 (2008) 125.

[25] R.C. Edgar, B.J. Haas, J.C. Clemente, C. Quince, R. Knight, UCHIME improves sensitivity and speed of chimera detection, Bioinformatics 27 (2011) 2194–2200.

[26] J.G. Caporaso, J. Kuczynski, J. Stombaugh, K. Bittinger, F.D. Bushman, E.K. Costello, N. Fierer, A.G. Pena, J.K. Goodrich, J.I. Gordon, G.A. Huttley, S.T. Kelley, D. Knights, J.E. Koenig, R.E. Ley, C.A. Lozupone, D. McDonald, B.D. Muegge, M. Pirrung, J. Reeder, J.R. Sevinsky, P.J. Tumbaugh, W.A. Walters, J. Widmann, T. Yatsunenko, J. Zaneveld, R. Knight, QIIME allows analysis of high-throughput community sequencing data, Nat. Methods 7 (2010) 335–336, http://dx.doi.org/10.1038/nmeth.f.303.

[27] R.C. Edgar, Search and clustering orders of magnitude faster than BLAST, Bioinformatics 26 (2010) 2460–2461, http://dx.doi.org/10.1093/bioinformatics/btq461.

[28] J.R. Cole, Q. Wang, E. Cardenas, J. Fish, B. Chai, R.J. Farris, A.S. Kulam-Syed-Mohideen, D.M. McGarrell, T. Marsh, G.M. Garrity, J.M. Tiedje, The ribosomal database project: improved alignments and new tools for rRNA analysis, Nucleic Acids Res. 37 (2009) D141–D145, http://dx.doi.org/10.1093/nar/gkn879.

[29] D. Pocaznoi, B. Erable, L. Etcheverry, M.-L. Delia, A. Bergel, Forming microbial anodes under delayed polarisation modifies the electron transfer network and decreases the polarisation time required, Bioresour. Technol. 114 (2012) 334–341.

[30] M. Mehanna, R. Basseguy, M.-L. Delia, A. Bergel, Role of direct microbial electron transfer in corrosion of steels, Electrochem. Commun. 11 (2009) 568–571, http://dx.doi.org/10.1016/j.elecom.2008.12.019.

[32] R.M. Hartline, D.F. Call, Substrate and electrode potential affect electrotrophic activity of inverted bioanodes, Bioelectrochemistry 110 (2016) 13–18, http://dx.doi.org/10.1016/j.bioelechem.2016.02.010.

[33] T. Ishii, S. Kawaichi, H. Nakagawa, K. Hashimoto, R. Nakamura, From chemolithoautotrophs to electrolithoautotrophs: CO_2 fixation by Fe(II)-oxidizing bacteria coupled with direct uptake of electrons from solid electron sources, Front. Microbiol. 6 (2015) 994, http://dx.doi.org/10.3389/fmicb.2015.00994.

[34] L. Jourdin, S. Freguia, B.C. Donose, J. Keller, Autotrophic hydrogen-producing biofilm growth sustained by a cathode as the sole electron and energy source, Bioelectrochemistry 102 (2015) 56–63, http://dx.doi.org/10.1016/j.bioelechem.2014.12.001.

[35] M.D. Yates, B.J. Eddie, N.J. Kotloski, N. Lebedev, A.P. Malanoski, B. Lin, S.M. Strycharz-Glaven, L.M. Tender, Toward understanding long-distance extracellular electron transport in an electroautotrophic microbial community, Energy Environ. Sci. 9 (2016) 3544–3558, http://dx.doi.org/10.1039/C6EE02106A.

[36] M.E. Lai, A. Bergel, Electrochemical reduction of oxygen on glassy carbon: catalysis by catalase, J. Electroanal. Chem. 494 (2000) 30–40, http://dx.doi.org/10.1016/S0022-0728(00)00307-7.

[37] K.-J. Chae, M.-J. Choi, J.-W. Lee, K.-Y. Kim, I.S. Kim, Effect of different substrates on the performance, bacterial diversity, and bacterial viability in microbial fuel cells, Bioresour. Technol. 100 (2009) 3518–3525, http://dx.doi.org/10.1016/j.biortech.2009.02.065.

[38] W.-R. Abraham, C. Strömpl, H. Meyer, S. Lindholst, E.R.B. Moore, R. Christ, M. Vancanneyt, B.J. Tindall, A. Bennasar, J. Smit, M. Tesar, Phylogeny and polyphasic taxonomy of *Caulobacter* species. Proposal of *Maricaulis* gen. nov. with Maricaulis maris (Poindexter) comb. nov. as the type species, and emended description of the genera *Brevundimonas* and *Caulobacter*, Int. J. Syst. Evol. Microbiol. 49 (1999) 1053–1073.

[39] J.-H. Yoon, S.-J. Kang, J.-S. Lee, H.W. Oh, T.-K. Oh, *Brevundimonas lenta* sp. nov., isolated from soil, Int. J. Syst. Evol. Microbiol. 57 (2007) 2236–2240.

[40] J.-H. Yoon, S.-J. Kang, J.-S. Lee, T.-K. Oh, *Brevundimonas terrae* sp. nov., isolated from an alkaline soil in Korea, Int. J. Syst. Evol. Microbiol. 56 (2006) 2915–2919.

[41] J.W. Zhang, E.R. Zhang, K. Scott, J.G. Burgess, Enhanced electricity production by use of reconstituted artificial consortia of estuarine bacteria grown as biofilms, Environ. Sci. Technol. 46 (2012) 2984–2992.

[42] V.R. Nimje, C.-Y. Chen, C.-C. Chen, J.-S. Jean, A.S. Reddy, C.-W. Fan, K.-Y. Pan, H.-T. Liu, J.-L. Chen, Stable and high energy generation by a strain of *Bacillus subtilis* in a microbial fuel cell, J. Power Sources 190 (2009) 258–263, http://dx.doi.org/10.1016/j.jpowsour.2009.01.019.